 CMC, vol.1, no.2, pp.191-204, 2004

Numerical Prediction of Dynamically Propagating and Branching Cracks Using Moving Finite Element Method

S. Tchouikov[1], T. Nishioka[1] and T. Fujimoto[1]

Abstract: Phenomena of dynamic crack branching are investigated numerically from a macroscopic point of view. Repetitive branching phenomena, interaction of cracks after bifurcation and their stability, bifurcation into two and three branches were the objectives of this research. For the analysis of dynamic crack branching, recently we developed moving finite element method based on Delaunay automatic triangulation [Nishioka, Furutuka, Tchouikov and Fujimoto (2002)]. In this study this method was extended to be applicable for complicated crack branching phenomena, such as bifurcation of the propagating crack into more than two branches, multiple crack bifurcation and so on. The switching method of the path independent dynamic J integral, which was developed for the case of simple two cracks branching phenomena, demonstrated it's excellent applicability also for the case of complicated crack branching. The simulation results are discussed with consideration to the experimental findings.

keyword: Dynamic crack bifurcation, dynamic fracture, crack propagation and arrest, moving finite element method, dynamic J integral, fracture prediction criteria, multiple branching.

1 Introduction

When dynamic fracture occurs in brittle materials and constructions it is rarely takes place as a propagation of a single crack. Conversely very often, single crack bifurcates into two or more cracks, which propagate simultaneously. Some of them branch again, others propagate as a single crack or arrest. Several propagating cracks interact and influence each other. The prediction of brittle fracture is very important problem in dynamic fracture mechanics. The accurate prediction of such complicated failure process is extremely important not only for academic interest, but also for safety design of constructions or for controllable dynamic destruction.

The dynamic crack bifurcation problem still remains as one of the most important unsolved problems in dynamic fracture mechanics. The problem of governing condition of dynamic crack branching is investigated in our recent experimental studies [Nishioka, Kishimoto, Ono and Sakakura (1999a, 1999b)]. The experiments on dynamic crack branching phenomena in Homalite-911 and Homalite-100 revealed, that the energy flux per unit time into a propagating crack tip or into a fracture process zone governs the dynamic crack branching. Other experimental investigations on evaluation of dynamic crack branching by method of caustics have been also performed recently [Nishioka, Matsumoto, Fujimoto and Sakakura (2003)].

There are some difficulties that must be overcome to perform accurate numerical simulation of dynamic crack bifurcation. In previous studies, the authors [Nishioka, Furutuka, Tchouikov and Fujimoto (2002)] developed a moving finite element method based on Delaunay automatic triangulation [Sloan and Houlsby (1984), Taniguchi (1992)], which satisfied the numerical requirements for simulation of two branches dynamic crack bifurcation phenomena. In present work this method is extended to simulate the dynamic crack branching into more than two branches, propagation of interacting cracks, multiple crack branching phenomena etc. In this method, the moving singularities at the tips of dynamically propagating cracks are treated accurately; even complicated fracture path is carefully generated and the fracture parameters, such as dynamic J integral and dynamic stress intensity factors are accurately evaluated even immediately after the bifurcation.

The propagation direction of each individual crack is controlled by local symmetry criterion. According to this criterion it was possible to find the propagation direction for two or three branches even immediately after crack

[1] Simulation Engineering Laboratory, Faculty of Maritime Sciences, Kobe University, Higashinada-Ku, Kobe, 658-0022, Japan

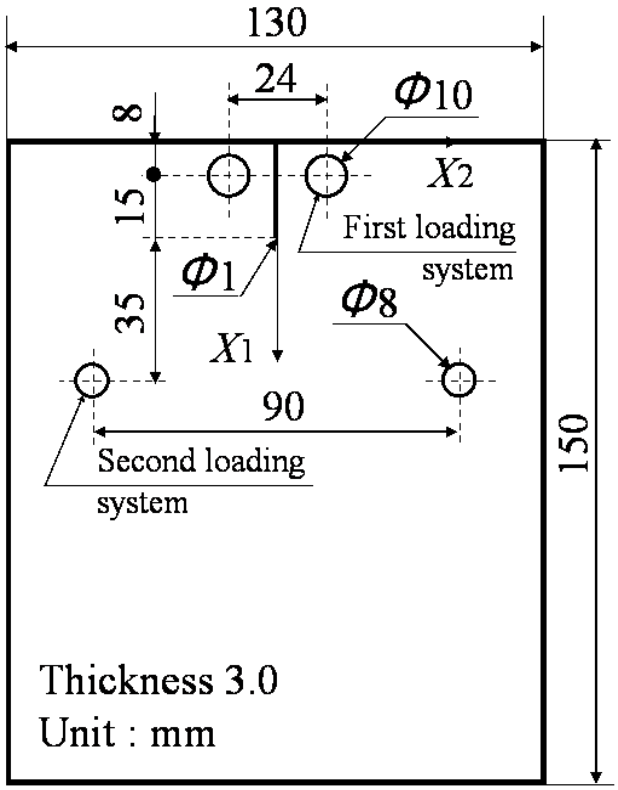

Figure 1 : Specimen geometry

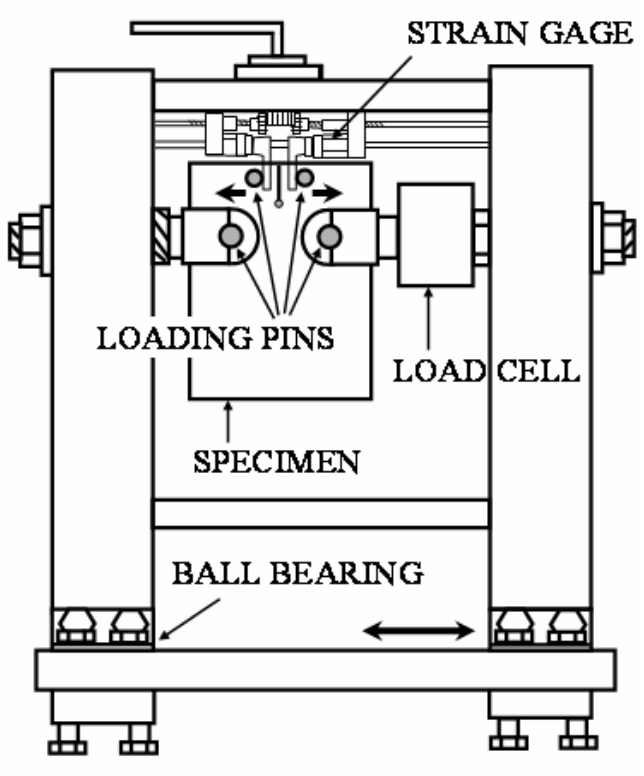

Figure 2 : Loading equipment

bifurcation. For crack growth predicting a unique dependence of dynamic fracture toughness on the crack speed only is assumed. For predicting of branching instant, at which dynamically propagating crack bifurcates, the critical amount of energy flux per unit time into a process zone is assumed.

2 Experimental Measurements

The experimental investigations of dynamic crack branching [Nishioka, Kishimoto, Ono and Sakakura (1999a, 1999b); Nishioka, Matsumoto, Fujimoto and Sakakura (2003)] were performed with major point of interest in under what conditions the crack branching occurs. In these experiments transparent material Homalite-911 was used. The material properties are as follows: Young's modulus E=2.15GPa, Poisson ratio ν=0.38 and mass density ρ=1281 kg/m^3. The geometry of a typical specimen used for fast crack branching test is shown in Fig.1. In the experiments crack initiates from a blunt notch, which length was set as 23mm from upper end of the specimen. The notch-root diameter is about 0.5 mm.

Two sets of displacement-controlled loads were applied to the specimen through two pairs of loading pins as shown in Fig.2. First, the some load P_2 was applied to the lower loading system and held constant. It produces a strong tensile stress field to supply enough energy into the propagating crack tip for crack branching. Then the upper loading system was gradually loaded by the L shape jigs as shown in Fig.2, until dynamic crack propagation occurred. The crack tries to bifurcate near the lower loading line. Examples of the high-speed photographs of the caustic patterns, which were recorded in the experiments, using a high-speed camera (with maximum framing rate two million frames per second) are shown in Fig.3. Measuring the crack-tip positions in each frame each crack propagation history was described by a polynomial curve. Then, differentiating the polynomials with time, the crack velocities were determined. From dimensions of the caustics patterns in photographs the experimental K values can be obtained by the method of caustics.

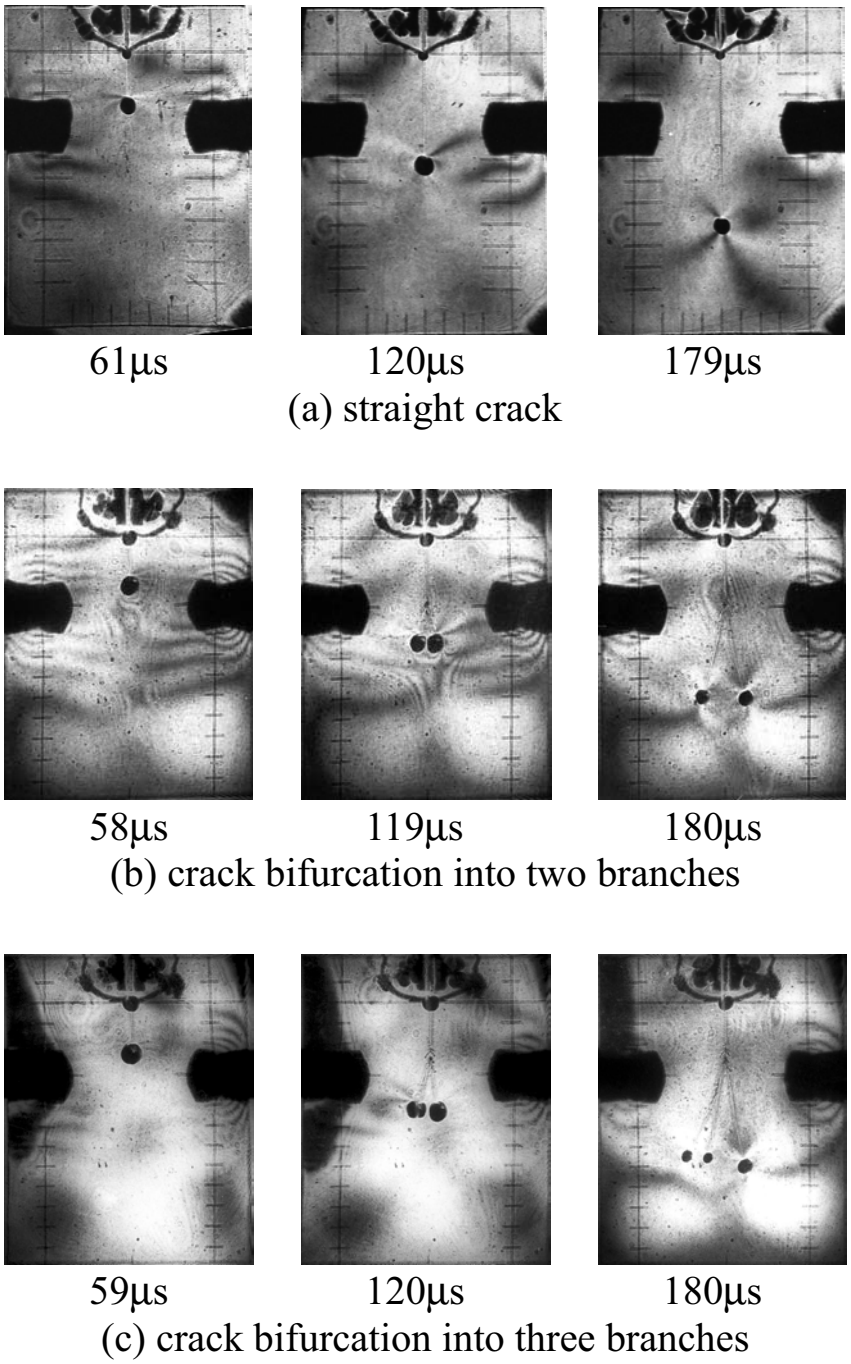

Figure 3 : High-speed photographs of dynamic fracture

3 Numerical Procedures

3.1 Moving Finite Element Method

Recently, for modeling of the crack propagation many innovative techniques have been developed, such as: the cell method [Ferretti (2003)], the novel non-hypersingular time-domain traction boundary element method [Zhang and Savaidis (2003)], the symmetric Galerkin boundary element method [Han and Atluri (2002)], the material point method [Nairn (2003)].

To simulate the crack propagation by the finite element

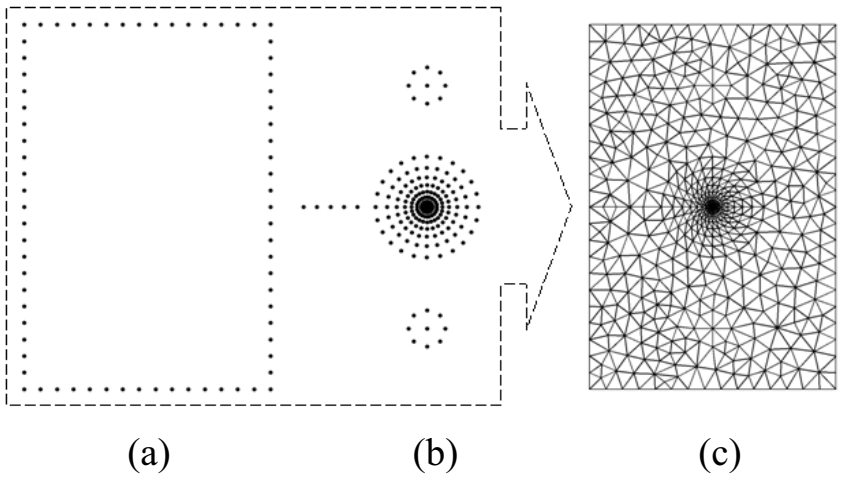

Figure 4 : An example of automatic mesh generation (a) exterior boundary points, (b) specified interior points, (c) generated mesh pattern

method, two different concepts of computational modeling can be considered, i.e., the stationary element procedure (or fixed element procedure), and the moving element procedure. [Nishioka and Atluri (1986), Nishioka (1994, 1997)]. Due to some disadvantages of the fixed element procedure we used the moving element procedure, which allowed us to accurately model the dynamically propagating [Nishioka, Tokudome, Kinoshita and Nishida (1998); Nishioka, Tokudome and Kinoshita (2001)] and branching crack [Nishioka, Furutuka, Tchouikov and Fujimoto (2002)].

In this study for mesh generation we used the modified Delaunay automatic triangulation [Taniguchi (1992)], which requires only exterior, interior boundary points and specified interior points (if they are necessary) (Fig.4). In consideration of the stress singularity each propagating crack tip is always surrounded by the specified interior points.

At the Delaunay automatic mesh generation stage the two surfaces of crack path have common nodal points, and the crack surfaces are described by element boundaries. In order to distinguish both surfaces of crack after Delaunay automatic mesh generation, dual nodes setting on crack path is used, so that, the nodal points with the same coordinates are have different numbers if there are lying on opposite crack surfaces. Therefore, the total number of nodal points increases and the element-nodes relations are changed. During crack propagation, when crack length is increased more than certain value, new nodal points are placed on crack path behind the group of surrounding interior points. Furthermore, only an area of the group of specified interior points with its neighborhood is actually re-meshing during crack propagation, the rest of the mesh pattern is remaining fixed for more accuracy of analysis.

For the time integration of the finite element equation of motion the Newmark method is used. To fulfill the unconditionally stable condition the Newmark's parameters are chosen to be β=1/4 and δ=1/2 [Bathe and Wilson (1976)]. For further details about time integration procedures please refer to [Nishioka, Furutuka, Tchouikov and Fujimoto (2002)].

3.2 Evaluation of Fracture Mechanics Parameters

In this study, to evaluate various fracture mechanics parameters for a dynamically propagating and branching cracks the path independent dynamic J integral derived by Nishioka and Atluri (1983) is used.

For most numerical analyses, considering dynamically propagating crack in an elastic solid, the global-axis components of the dynamic J integral (J') can be evaluated by the following expression:

$$J'_k = \int_{\Gamma+\Gamma_c} [(W+K)n_k - t_i u_{i,k}]dS + \int_{V_\Gamma} [(\rho\ddot{u}_i - f_i)u_{i,k} - \rho\dot{u}_i\dot{u}_{i,k}]dV \quad (1)$$

where u_i, t_i, f_i, n_k and ρ denote the displacement, traction,

body force, outward direction cosine, and mass density, respectively. W and K are the strain and kinetic energy densities, respectively, and $()_{,k} = \partial()/\partial X_k$. The integral paths $\Gamma_\varepsilon, \Gamma$ and the Γ_c shown in Fig.5 denote a near-field path, far-field path and crack surface path, respectively. V_Γ is the region surrounded by Γ, while V_ε is the region surrounded by Γ_ε.

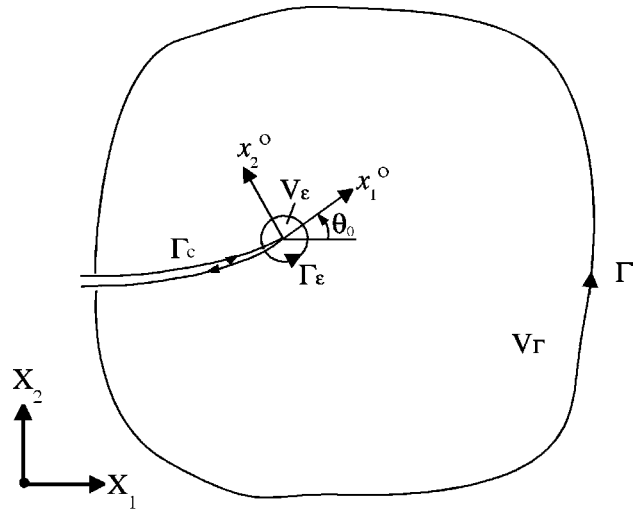

Figure 5 : Definition of integral paths

The crack-axis components of the dynamic J integral can be evaluated by the following coordinate transformation:

$$J_l'^0 = \alpha_{lk}(\theta_0) J_k', \tag{2}$$

where α_{lk} is the coordinate transformation tensor and θ_0 is the angle between the global X_1 and the crack axis x_1^0.

For the elastodynamically propagating crack with velocity C the dynamic J integral can be related to the instantaneous stress intensity factors as in [Nishioka and Atluri (1983)]:

$$J_1'^0 = \frac{1}{2\mu}\{A_I(C)K_I^2 + A_{II}(C)K_{II}^2 + A_{III}(C)K_{III}^2\} \tag{3}$$

$$J_2'^0 = -\frac{A_{IV}(C)}{\mu} K_I K_{II} \tag{4}$$

where μ is the shear modulus, and $A_I(C) - A_{IV}(C)$ are functions of crack velocity C and given in [Nishioka and Atluri (1983)].

The dynamic J integral has following salient features:

(i) It physically represents the dynamic energy release rate G [Nishioka and Atluri (1983)].

(ii) For the far-field path, it has the property of the path-independent integral [Nishioka and Atluri (1983)].

(iii) For the near-field path, it is practically invariant with the shape of the infinitesimal near-field path [Nishioka (1994)].

(iv) The dynamic J integral includes the static J integral for elastostatic fracture problems.

(v) The near-field path can be taken as the boundary of a fracture process zone (if it is known a priori).

To accurately evaluate the inplane mixed-mode stress intensity factors from the dynamic J integral values, the component separation method [Nishioka (1994)] was proposed. If the energy release rate G or the crack-axis component is obtained by Eq.(2), the formulae of the component separation method can be expressed as:

$$\begin{aligned} K_I &= \delta_I \left\{ \frac{2\mu J_1'^0 \beta_2}{A_I(\delta_I^2\beta_2 + \delta_{II}^2\beta_1)} \right\}^{1/2} \\ &= \delta_I \left\{ \frac{2\mu G \beta_2}{A_I(\delta_I^2\beta_2 + \delta_{II}^2\beta_1)} \right\}^{1/2} \end{aligned} \tag{5}$$

$$\begin{aligned} K_{II} &= \delta_{II} \left\{ \frac{2\mu J_1'^0 \beta_2}{A_{II}(\delta_I^2\beta_2 + \delta_{II}^2\beta_1)} \right\}^{1/2} \\ &= \delta_{II} \left\{ \frac{2\mu G \beta_2}{A_{II}(\delta_I^2\beta_2 + \delta_{II}^2\beta_1)} \right\}^{1/2} \end{aligned} \tag{6}$$

Some of the features of the component separation method are: (i) mixed-mode stress intensity factors can be evaluated by ordinary non-singular elements, and (ii) the signs of $K_I$and K_{II} are automatically determined by the signs of δ_I and δ_{II}, respectively.

Because of difficulty in setting far-field integral path separately for each just bifurcated crack tip, a switching method of the path independent dynamic J integral was proposed [Nishioka, Furutuka, Tchouikov and Fujimoto (2002)]:

$$\begin{aligned} J_k' = &\int_{\Gamma+\Gamma_C} [(W+K)\, n_k - t_i u_{i,k}] s dS \\ &+ \int_{V_\Gamma} [\{(\rho\ddot{u}_i - f)\, u_{i,k} - \rho\dot{u}_i\dot{u}_{i,k}\} s dV \\ &+ \sigma_{ij} u_{i,k} s_{,j} - (W+K)\, s_{,k}] dV \end{aligned} \tag{7}$$

where Γ is a far-field integral path, that encloses all branched crack tips and s is a continuous function defined in V_Γ (Fig.6).

For calculation of the dynamic J integral for certain crack tip the s function is set as s=1 for the point at that crack tip and for the points in whole domain V_Γ and s=0 for the points at the others crack tips. Equation (7) made possible accurate evaluation of the dynamic J integral components for interacting branched crack tips.

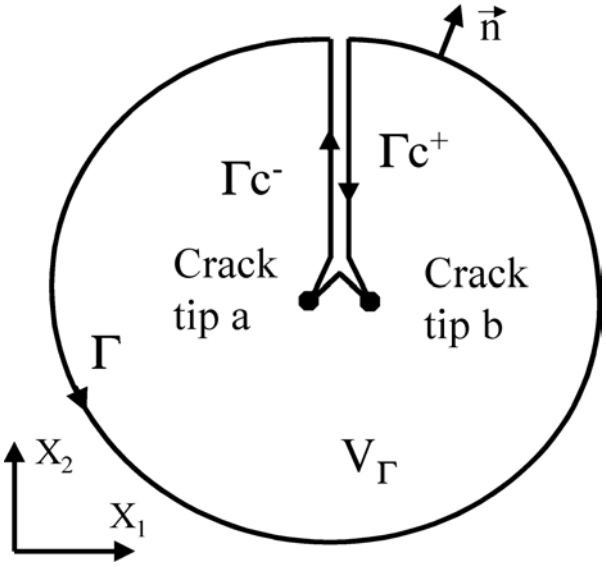

Figure 6 : Integral path for branched crack tips

3.3 Fracture Path Prediction Criterion

Many propagation-direction criteria have been proposed before. They can be divided into two groups: explicit prediction theories and implicit prediction theories. An explicit prediction theory predicts the propagation direction satisfying the postulated criterion based on a physical quantity for the current crack tip. Contrary, an implicit prediction theory seeks the propagation direction that satisfies the postulated criterion based on physical quantity after the crack is advanced with a small crack-length increment. It is known that in general the implicit prediction theories are more accurate, although an iterative process usually is needed to find the propagation direction.

In this study the propagation direction of each individual crack is predicted accordingly to a local symmetry criterion [Goldstein and Salganik (1974)], which falls into the group of implicit prediction theories. The fracture path is predicted in an iterative manner as follows. At a generic time step n, as a first trial, the crack is advanced in the tangential direction $\theta_n^{(i)}$ (i=1) equal to a crack tip direction at the previous step n-1. If mode II stress intensity factor K_{II} is almost zero at the attempted crack-tip location, the crack is advanced in this direction $\theta_n^{(i)}$. If the K_{II} value is not zero, the crack is tentatively advanced in the direction of $\theta_n^{(i+1)} = \theta_n^{(i)} + \Delta\theta$ and $\theta_n^{(i+2)} = \theta_n^{(i)} - \Delta\theta$ as the next two trials. Each time the satisfaction of the criterion at the trial crack tip location is checked. If the criterion is not satisfied in both cases the next trial direction is calculated accordingly to the square polynomial curve fitting all K_{II} values versus $\theta_n^{(i)}$(i=1,2,...) of previous trials. These procedures are repeated until the criterion is satisfied for each propagating crack.

Furthermore, when using the local symmetry principle it is possible to find propagation direction of each crack immediately after bifurcation in case of two and three cracks branching.

3.4 Crack Growth Prediction Criterion

In fast fracture mechanics, for dynamically propagating cracks under quasi-static as well as dynamic loading conditions, it has been suggested that

$$K = K_D(T, C, \dot{C}, ...) \tag{8}$$

where K_D is the dynamic propagation fracture toughness. Effects of crack acceleration and deceleration are still not fully clarified and under investigation [Takahashi and Arakawa (1987), Nishioka, Syano and Fujimoto (2000)]. Furthermore, several works [Gates (1980), Kalthoff, Beinert and Winkler (1981), Nishioka, Kishimoto, Ono, Sakakura (1991a)] have reported the geometry-dependence of K_D.

According to the criterion given by Eq.(8), crack arrest occurs when the stress intensity factor becomes smaller than or equal to a critical value. This can be expressed as

$$K \leq K_D(0) \equiv K_a^{dyn} \equiv K_A \tag{9}$$

where K_a^{dyn} or K_A denotes the dynamic crack arrest toughness. The superscript "dyn" is used to distinguish a material property from the so-called static arrest toughness K_a (K_a^{sta}).

In this study, we assume a unique dependence of dynamic fracture toughness on the crack tip speed only [Dally, Fourney and Irwin (1985)]. For establishing crack growth prediction criterion, we choused three experimental results, in which crack propagated straightly without branching [Nishioka, Matsumoto, Fujimoto and Sakakura (2003)]. The dynamic propagation toughness $K_D(C)$ in each case was different. The K_A value for each experiment was different and was calculated by interpolating $K_D(C)$ on C=0. Nominal dynamic stress intensity factors are defined by K_A for each experiment. A phenomenological relation between nominal stress intensity factor and nominal crack tip speed was derived from three experimental results (see Fig.7).

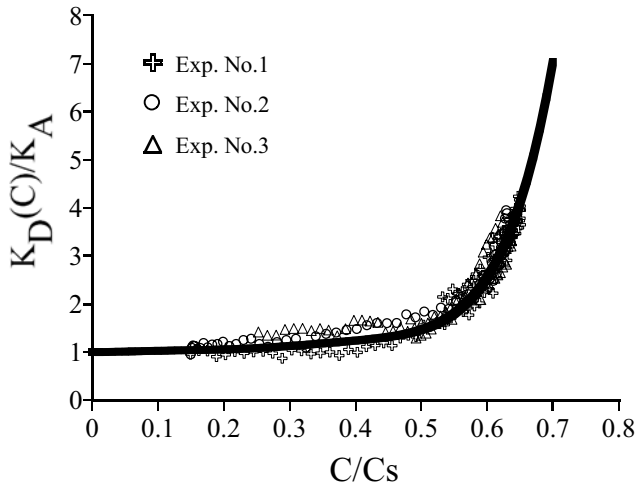

Figure 7 : Dynamic fracture toughness for Homalite-911 (C: crack tip speed, Cs: shear wave speed)

Using K_A value for each of three experiments a phenomenological relation shown in Fig.7 was obtained.

In the experiments, due to specimen geometry, as load P_1 was meant to just initiate crack, the lower loading P_2 value was most influential on the crack propagation and branching. For experimental lower loading P_2 and initial conditions of each experiment, calculating K_Q – a mode I stress intensity factor for the initial crack under quasi-static loading for various upper loading P_1, a relation between P_2/P_1 and K_Q/K_A was obtained (Fig.8).

Fracture initiation for static loading configurations is strongly dependent on the initial crack tip radius. In this study, we are basing on the experiments in which the initial notch-root diameter was about 0.5mm. Therefore, for

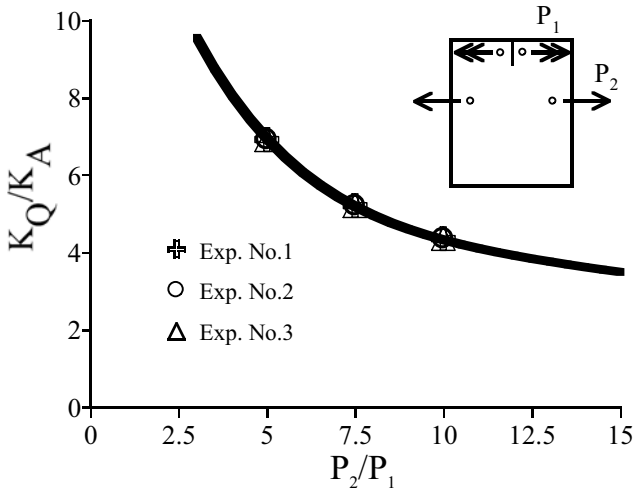

Figure 8 : The relation between dynamic crack arrest toughness K_A, initiation quasi-static K_Q and loading conditions for used specimen geometry

initiation under quasi-static loading from a blunt notch, the K_I must reach some critical quasi-static stress intensity K_Q value, which is assumed as $K_Q = 1.75[Pa\sqrt{m}]$.

In numerical analysis, first a certain load P_2 and very small load P_1 is statically applied to both loading systems. Then K_I, calculated for the initial crack tip, is compared with the assumed K_Q value. If K_I is less than K_Q, upper load P_1 is gradually increased until K_I reaches K_Q. When value of K_I becomes more or equal K_Q, knowing P_2/P_1 and K_Q, the dynamic crack arrest toughness K_A for choused specimen is determined from curve in Fig.8. At the static analysis under the fracture loads, the displacements at the loading points were evaluated and these were used as the prescribed displacement in the finite element model after crack initiation. For each individual crack tip, crack speed is predicted by iteration process, so that K_I of crack tip propagating with velocity C is always equal $K_D(C)$ (Fig.7).

3.5 Crack branching criterion

The determination of crack branching instant (i.e. where and when propagating crack bifurcates) is very important problem in the dynamic fracture prediction studies. Branched cracks are often observed in brittle materials and structures. Many attempts have been made in order to clarify the mechanism of crack branching. However the governing condition for dynamic cracks branch-

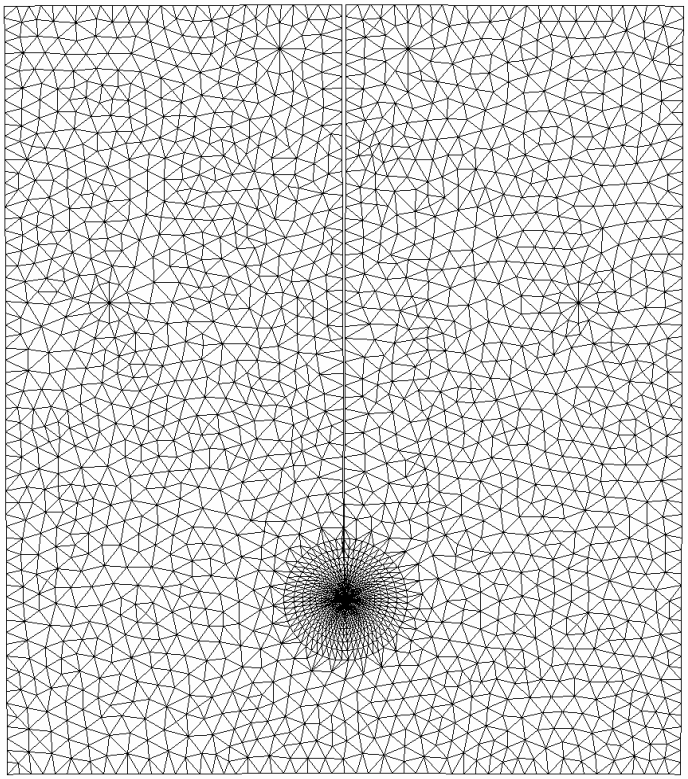

Figure 9 : Deformed mesh pattern for straight crack propagation (P_2=1.4kN)

ing had not been fully elucidated until our recent experimental studies [Nishioka, Kishimoto, Ono and Sakakura (1999a, 1999b)]. The experimental results revealed, that the energy flux per unit time into a propagating crack tip or into a fracture process zone, which can be expressed as:

$$\Phi_{total} = J_1' \cdot C, \tag{10}$$

governs the dynamic crack bifurcation. In this study we assumed crack branching to take place at a given critical Φ^c_{total}=550 [J/ms]. Furthermore, we suggested two branching cases: into two and three branches.

4 Results

The input data, such as specimen geometry, material properties, nodes number, values of critical fracture parameters, was set the same for all numerical examples, except only load P_2, which was set 1.4kN, 1.6kN, 1.8kN and 2.0kN. In each loading case two possibilities of crack bifurcation were suggested: two and three macro-cracks branching.

In numerical simulations, first, the static analysis under the fracture loads was performed. The displacements at the loading points were evaluated and these values were used as the prescribed displacement in the finite element model after crack initiation. The time increment of $\Delta t = 2\mu s$ was used.

As the upper loading device can only "push" the loading pins but not "pull", the fixed boundary conditions at the upper loading points in the numerical analysis may lead to a spurious deformation behavior of the specimen. Thus, the possibility of lack of contact of the L shape jigs with the loading pins should be taken in account. In present study, to solve this problem, the contact/non-contact boundary conditions [Nishioka, Perl and Atluri (1983); Nishioka and Atluri (1982); Nishioka, Furutuka, Tchouikov and Fujimoto (2002)] are employed in the numerical simulations.

The deformed mesh pattern for case of load P_2=1.4kN is shown in Fig.9. The initial number of elements and number of nodes were 6756 and 3500 respectively.

The time variations of the dynamic stress intensity fac-

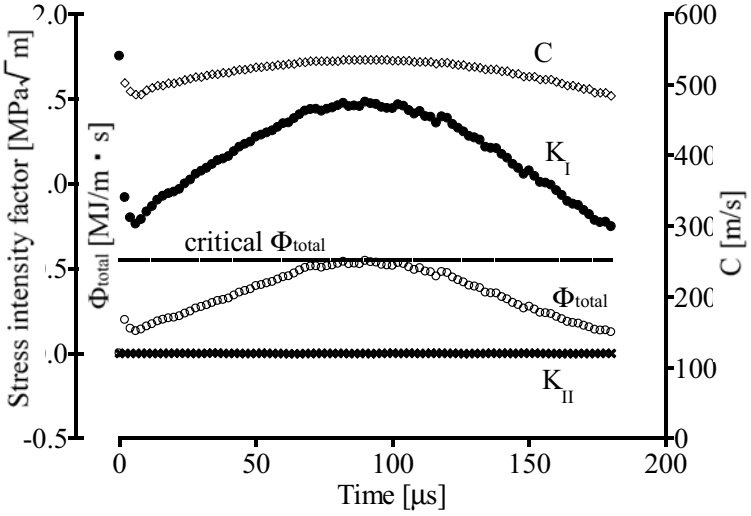

Figure 10 : Variations of dynamic SIF, energy flux and crack velocity C for not bifurcated crack (P_2=1.4kN)

tors, energy flux to the propagating crack tip per unit time and predicted crack speed are plotted in Fig.10. The Φ_{total} of propagating crack did not reached a critical value, so there was just a straight crack propagation without bifurcation. After crack starts propagate the K_I value drops for about a half of K_Q and then increases until crack reaches lower loading line area. The crack propagation speed was in interval 490-535m/s which is more then 0.6Cs.

The deformed mesh patterns for load P_2 equal 1.6kN, 1.8kN and 2.0kN are shown in Fig.11. Two types of crack branching was assumed: into two and three branches. For loading of 1.6kN and 1.8kN crack branching occurred only once. The location of crack branching is closer to initial crack for larger lower loading. In case of lower loading 2.0kN for both types a multiple crack branching occurred. For case of two cracks branching both of the cracks branched again symmetrically and did not stop. For three branches case only a central crack branched again. Finally for branching into three cracks both sides cracks arrested and only a central crack continued propagation. Due to random mesh and piling of calculations a slight asymmetry effects can be noticed. Furthermore, the contact/non-contact problem for crack surfaces was ignored in this study, so a small overlapping can be seen for three branches case. For multiple three branches case, shown in Fig.11(c), due to five crack tips propagating simultaneously, the number of elements and nodes increased exceedingly and was 20038 and 10378 respectively.

The computed variations of input (E), strain (W), kinetic (K) and fracture (F) energies with time for two and three branches with load 1.6kN are shown in Fig.12. It should be noted that in the present procedure, each of the quantities E, W, K and F is calculated separately and directly. Thus, the fact that W+K+F is almost equal to E at all times is an inherent check on the accuracy of the calculation. It also can be seen that for three branches case the fracture energy F is slightly larger than fracture energy for two branches case.

Even immediately after crack branching the values of dynamic J integral were accurately calculated. The path independence of dynamic J integral for central branched crack tip in case of 1.6kN loading is shown in Fig.13.

The dynamic stress intensity factors for (a) two and (b) three branches with loading of 1.6kN are plotted in Fig.14. Due to the local symmetry criterion choused for path prediction, mode II stress intensity factors are almost zero for all propagating cracks throughout the analysis. The mode I SIF for central crack in Fig.14(b) is much larger then K_I of two others cracks, especially at the final stage of simulations. Finally all cracks on sides arrested, and only the central crack continued propagating.

The variations of energy flux to the propagating crack tips per unit time for 1.6kN loading are plotted in Fig.15. It can be seen, that when the energy flux for straightly propagating crack becomes larger a critical value crack

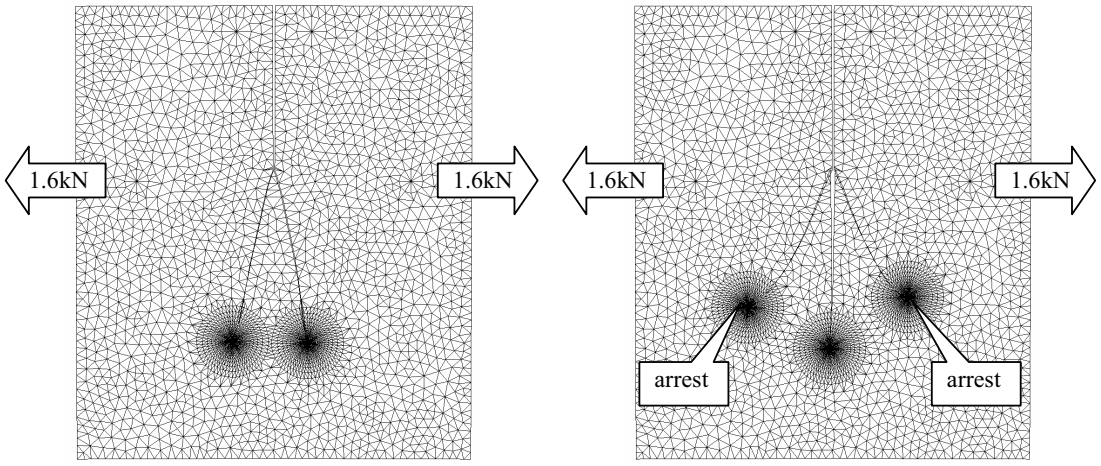

(a) lower loading P_2=1.6kN

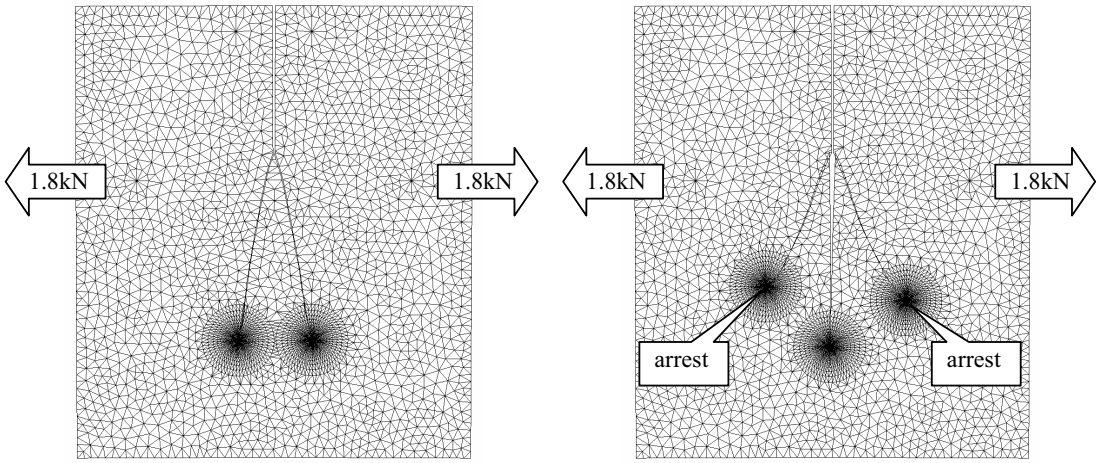

(b) lower loading P_2=1.8kN

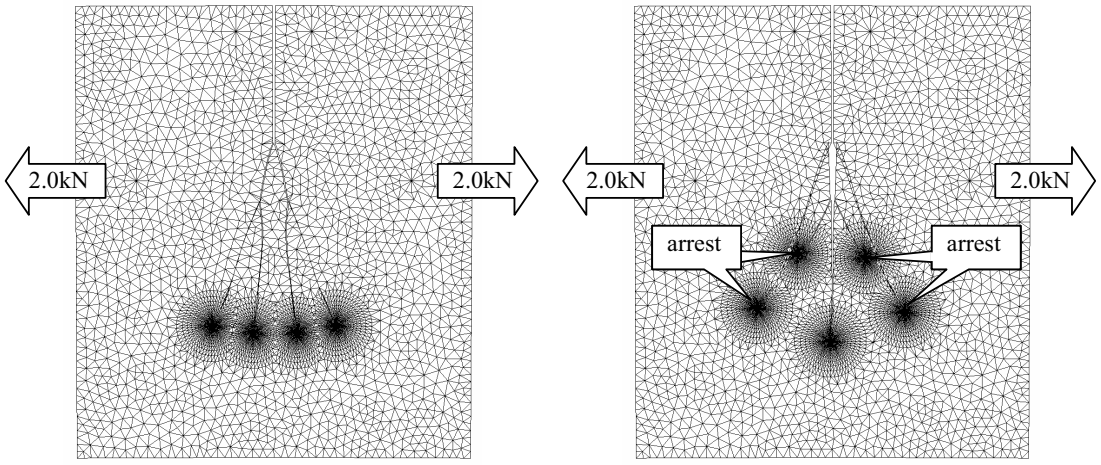

(c) lower loading P_2=2.0kN

Figure 11 : Deformed mesh patterns for crack branching into two and three branches with different lower loading $(180\mu s)$

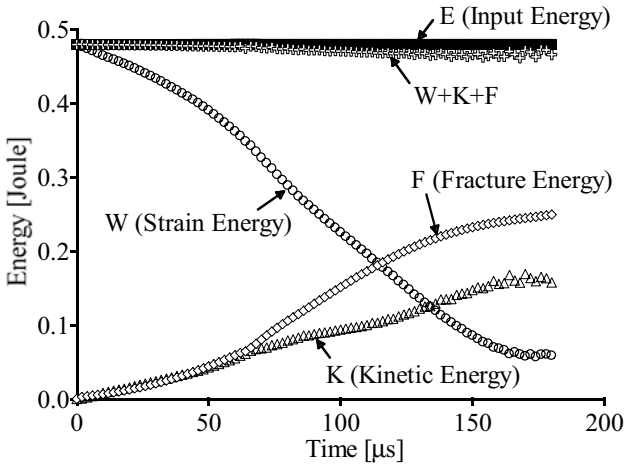

(a) two branches

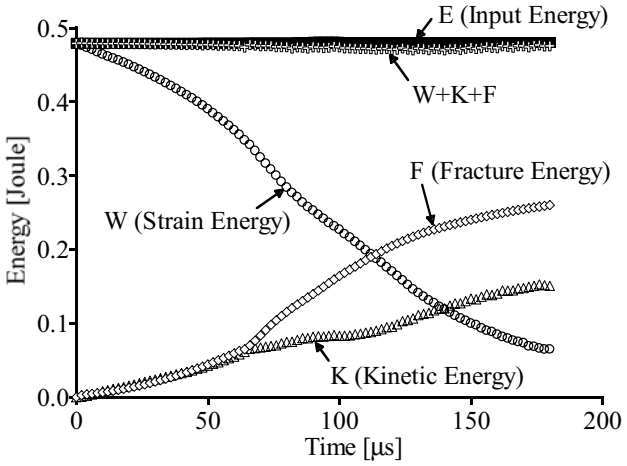

(b) three branches

Figure 12 : Energy balance (P_2=1.6kN)

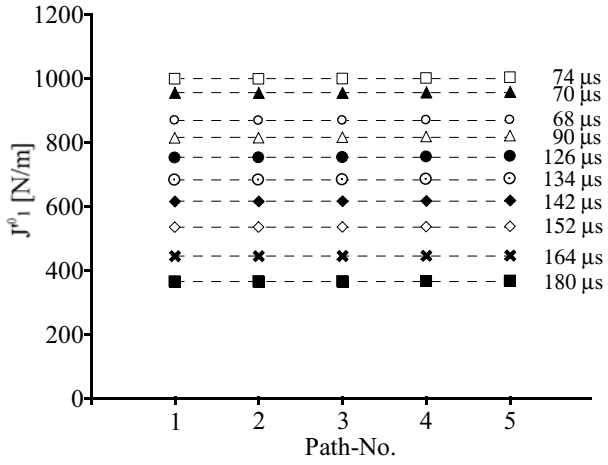

Figure 13 : Dynamic J integral against path number (P_2=1.6kN, central crack of three branches)

bifurcation occurred. In this loading case energy flux for all branched cracks did not reach a critical value again, so multiple branching did not occur. It also can be seen, that a sum of energy flux for branched cracks is much larger for three cracks branching at the early stage after branching.

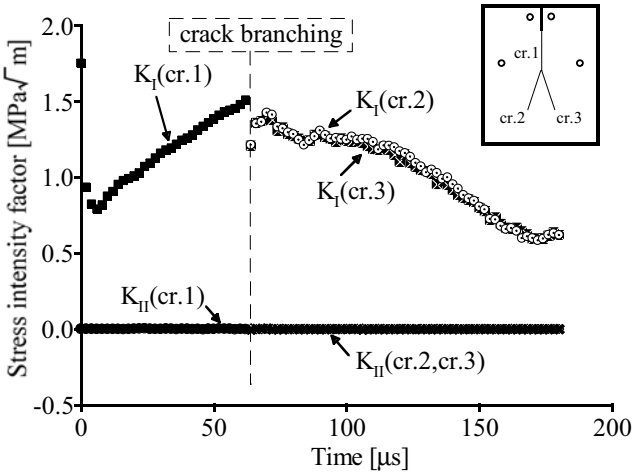

(a) two branches

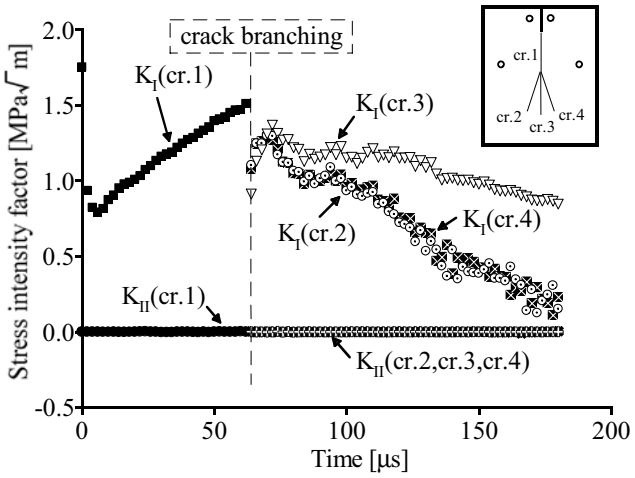

(b) three branches

Figure 14 : Variations of dynamic SIF (P_2=1.6kN)

The energy flow through a contour Γ with normal vector n_j to the crack tip can be expressed as follows:

$$\Phi = -\int_{\Gamma} \varphi_j n_j dS \tag{11}$$

where

$$\varphi_j = -C \cdot [(W+K)\delta_{1j} - \sigma_{ij} u_{i,1}] \tag{12}$$

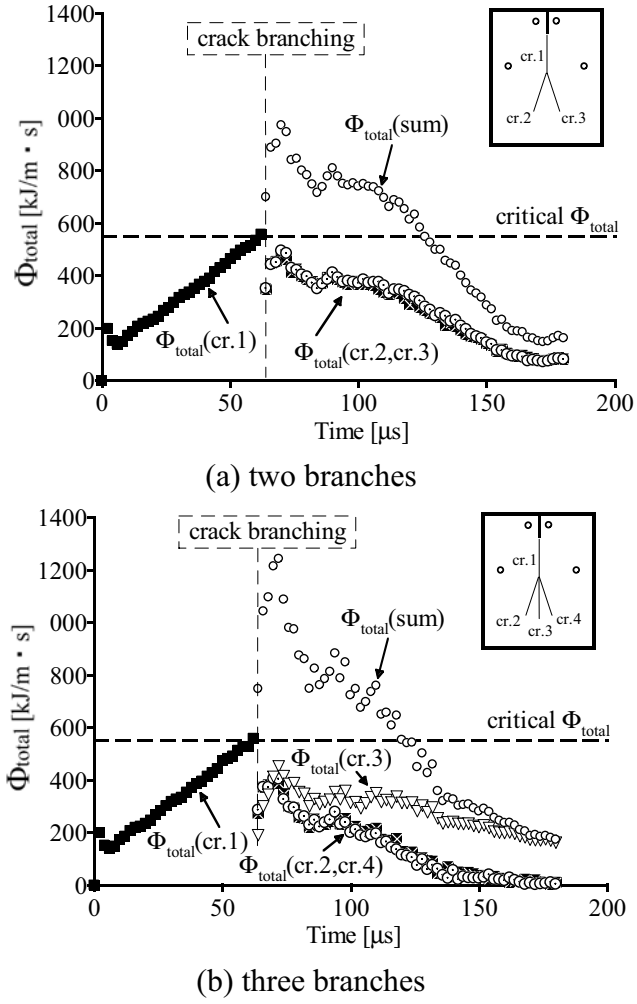

Figure 15 : Variations of energy flux (P_2=1.6kN)

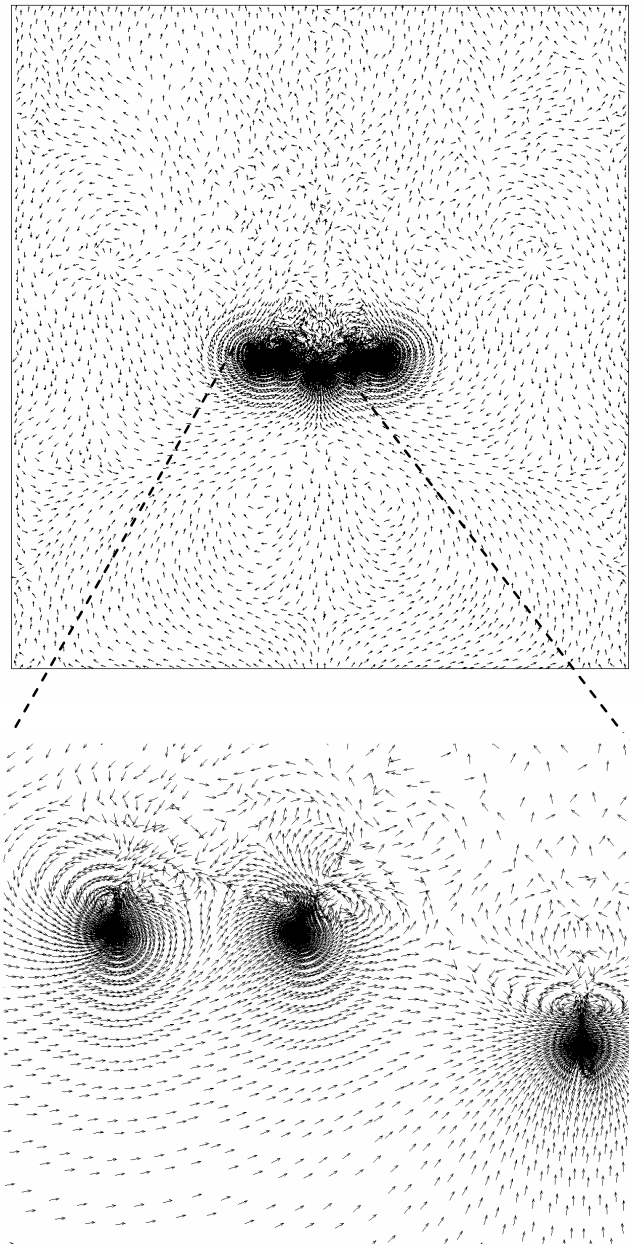

Figure 16 : The orientation of the energy flux vector ($P_2 = 2.0$kN, multiple three branches)

The sign in Exp.(12) is chosen so that the vector φ_j pointing toward the crack tip corresponds to an energy flux into the crack tip. The orientation of the energy flux vector for whole specimen and in the vicinity of the propagating cracks after bifurcation for loading case 2.0kN, three branches type is shown in Fig.16. The energy flux in front of central crack is oriented toward the propagating crack tip but in front of side cracks it is oriented to a central propagating crack, especially for crack between central crack and farthest left side crack. This explains why finally all sides crack have arrested while central crack continued propagating.

The simulation results (for loading 1.6kN) in comparison with actually fractured specimens are shown in Fig.17. The predicted fracture paths are very similar with experimental ones. For three branches type as in experiments, both side cracks have arrested while central crack continued propagating. For two branches type there was no crack arrest.

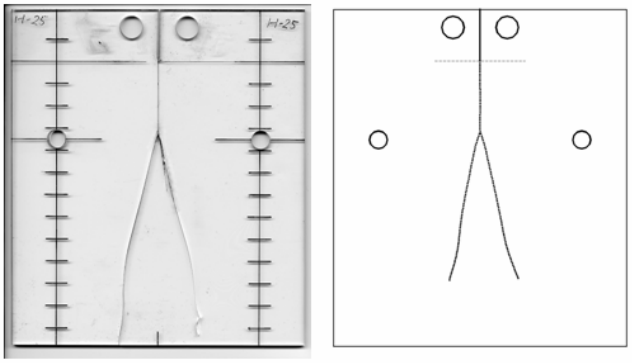

experiment prediction
(a) two branches

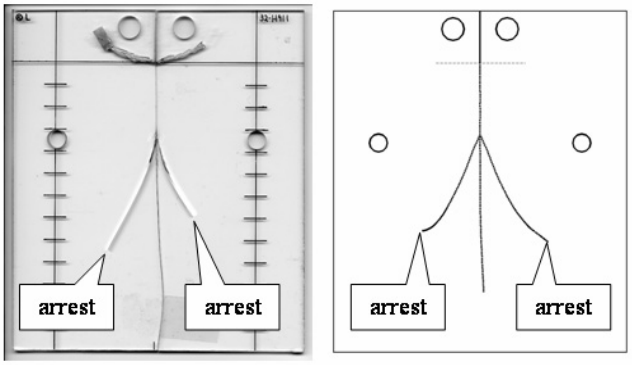

experiment prediction
(b) three branches

Figure 17 : Examples of fractured specimen and prediction results

5 Conclusions

In this study, the moving finite element method based on Delaunay automatic triangulation was further developed for the numerical simulation of complicated dynamic crack bifurcation phenomena, such as branching into two or three branches and multiple branching (i.e. each branch encounters branching and so on). Various dynamic fracture parameters were accurately evaluated by the switching method of the path independent dynamic J integral even immediately after crack bifurcation.

The dynamic bifurcation phenomena observed experimentally was successfully predicted by the numerical simulations with conjunction of the local symmetry criterion, the dynamic fracture toughness criterion and the critical energy flux criterion.

Acknowledgement: This work was supported by the grant from Japan Society for the Promotion of Science (No. 14011647), by the Grant-in-Aid for Scientific Research (No. 14205019) and by the Natural Science Grant from Mitsubishi Foundation.

References

Bathe, K. J.; Wilson, E. L. (1976): *Numerical methods in finite element analysis*. Prentice-Hall, New Jersey.

Dally, J. W.; Fourney, W. L.; Irwin, G. R. (1985): On the uniqueness of stress intensity factor – crack velocity relationship. *International Journal of Fracture*, vol.27, pp.159-168.

Ferretti, E. (2003): Crack Propagation Modeling by Remeshing Using the Cell Method (CM). *CMES: Computer Modeling in Engineering & Sciences*, vol.4, no.1, pp.51-72.

Gates, R. S. (1980): Some effects of specimen geometry on crack propagation and arrest. In: Hahn, G.T. and Kanninen, M.F. (eds) *"Crack Arrest Methodology and Applications"*, ASTM STP 711.

Goldstein, R. V.; Salganik, R. L. (1974): Brittle fracture of solids with arbitrary cracks. *International Journal of Fracture*, vol.10, pp.507-523.

Han, Z. D.; Atluri, S. N. (2002): SGBEM (for Cracked Local Subdomain) – FEM (for uncracked global Structure) Alternating Method for Analyzing 3D Surface Cracks and Their Fatigue-Growth. *CMES: Computer Modeling in Engineering & Sciences*, vol.3, no.6, pp.699-716.

Kalthoff, J. F.; Beinert, J.; Winkler, S. (1981): Analysis of fast running and arresting cracks by the shadow optical method of caustics. In: Sijthoff and Noordhoff (eds) *"Optical Methods in Mechanics of Solids"*.

Nairn, J. A. (2003): Material Point Method Calculations with Explicit Cracks. *CMES: Computer Modeling in Engineering & Sciences*, vol.4, no.6, pp.649-664.

Nishioka, T. (1994): The state of the art in computational dynamic fracture mechanics. *JSME International Journal*, Series A, vol.37, pp.313-333.

Nishioka, T. (1997): Computational dynamic fracture mechanics. *International Journal of Fracture*, vol.86, no.1/2, pp.127-159.

Nishioka, T.; Atluri, S. N. (1982): Finite element simulation of fast fracture in steel DCB specimen. *Engineer-*

ing Fracture Mechanics, vol.16, no.2, pp.157-175.

Nishioka, T.; Atluri, S. N. (1983): Path independent integrals, energy release rates and general solutions of near-tip fields in mixed-mode dynamic fracture mechanics. *Engineering Fracture Mechanics*, vol.18, no.1, pp.1-22.

Nishioka, T.; Atluri, S. N. (1986): Computational methods in dynamic fracture, In: S.N. Atluri (ed) *Computational methods in the mechanics of fracture*, Elsevier Science Publishers, pp.336-383.

Nishioka, T.; Furutuka, J.; Tchouikov, S.; Fujimoto, T. (2002): Generation-phase simulation of dynamic crack bifurcation phenomenon using moving finite element method based on Delaunay automatic triangulation. *CMES: Computer Modeling in Engineering & Sciences*, vol.3, pp.129-145.

Nishioka, T.; Kishimoto, T.; Ono, Y.; Sakakura, K. (1999a): Basic studies on the governing criterion for dynamic crack branching phenomena. *Transactions of the Japan Society of Mechanical Engineers*, vol.65, no.633, Ser. A, pp.1123-1131.

Nishioka, T.; Kishimoto, T.; Ono, Y.; Sakakura, K. (1999b): Governing criterion of dynamic crack bifurcation. In: F. Ellyin and J.W. Provan (eds.) *Progress in mechanical behaviour of materials*, Volume I, pp.255-260.

Nishioka, T.; Matsumoto, K.; Fujimoto, T.; Sakakura, K. (2003): Evaluation of dynamic crack bifurcation by method of caustic. *Journal of the Japanese Society for Experimental Mechanics*, vol.3, no.2, pp.21-28.

Nishioka, T.; Perl, M.; Atluri, S. N. (1983): An analysis of dynamic fracture in an impact test specimen. *Journal of Pressure Vessel Technology*, vol.105, no.2, pp.124-131.

Nishioka, T.; Syano. S.; Fujimoto, T. (2000): A study on crack acceleration and deceleration effects in dynamic fracture phenomena, *Proceedings of International Conference on Computational Engineering and Science*, Los Angeles, CA, USA, August 21-25, 2000.

Nishioka, T.; Tokudome, H.; Kinoshita, M.; Nishida, H. (1998): Dynamic fracture path prediction by moving finite element method based on Delaunay automatic triangulation. Modeling and simulation based engineering, vol. II, *Tech Science Press*, pp.1335-1340.

Nishioka, T.; Tokudome, H.; Kinoshita, M. (2001): Dynamic fracture-path prediction in impact fracture phenomena using moving finite element method based on Delaunay automatic mesh generation. *International Journal of Solids and Structures*, vol. 38, no.30-31, pp.5273-5301.

Sloan, S. W.; Houlsby, G. T. (1984): An implementation of Watson's algorithm for computing two-dimensional Delaunay triangulation. *Advances in engineering software*, vol.6, pp.192-197.

Takahashi, K.; Arakawa, K. (1987): Dependence of crack acceleration on the dynamic stress-intensity factor in polymers. *Experimental Mechanics*, vol.27, pp.195-200.

Taniguchi, T. (1992): *Automatic mesh generation for FEM: use of Delaunay triangulation*. Morikita Publishing.

Zhang, Ch.; Savaidis, A. (2003): 3-D Transient Dynamic Crack Analysis by a Novel Time-Domain BEM. *CMES: Computer Modeling in Engineering & Sciences*, vol.4, no.5, pp.603-612.